Am J Transl Res 2019;11(1):45-66
www.ajtr.org /ISSN:1943-8141/AJTR0086866

Original Article

Comprehensive clinical implications of homeobox A10 in 3,199 cases of non-small cell lung cancer tissue samples combining qRT-PCR, RNA sequencing and microarray data

Yi-Nan Guo[1*], Bin Luo[2*], Wen-Jie Chen[1], Xin Chen[2], Zhi-Gang Peng[2], Kang-Lai Wei[1], Gang Chen[1]

Departments of [1]Pathology, [2]Oncology, First Affiliated Hospital of Guangxi Medical University, Nanning 530021, Guangxi, Zhuang Autonomous Region, People's Republic of China. [*]Equal contributors.

Received October 16, 2018; Accepted December 18, 2018; Epub January 15, 2019; Published January 30, 2019

Abstract: In the current study, we proposed to explore the potential role and related signaling pathways of Homobox A10 (HOXA10) in non-small cell lung cancer (NSCLC). HOXA10 levels in lung adenocarcinoma (LUAD) and lung squamous cell carcinoma (LUSC) were detected by qRT-PCR and the expression of HOXA10 was significantly up-regulated in the NSCLC tissue of all 55 pairs (P = 0.037). Overexpression of HOXA10 was closely correlated with the clinical stage of LUSC (P = 0.011). HOXA10 expression in RNA sequencing data based on 1, 077 cases exhibited concordant significant up-regulation in NSCLC, LUAD and LUSC (P < 0.001). In NSCLC, HOXA10 expression was closely correlated to patient T stage (P = 0.006). In LUAD, HOXA10 expression was compactly correlated to patient N stage (P = 0.02). Some of the microarrays from Gene Expression Omnibus (GEO) and ArrayExpress showed consistent over-expression of HOXA10 levels in NSCLCs. More importantly, the combined SMD value was 0.052 (95% CI: 0.29-0.75, P < 0.001) generated by meta-analysis from 47 datasets based on 4, 616 cases of NSCLC. The area under the curve (AUC) of SROC supported the over-expression of HOXA10 in NSCLC as being 0.88 (95% CI: 0.81-0.93), with sensitivity and specificity of 0.88 (95% CI: 0.81-0.93) and 0.56 (95% CI: 0.44-0.66), respectively. In addition, 111 co-expressed genes were collected from cBioPortal and enriched in "cell cycle", "cell adhesion molecules", "p53 signaling", and "adherens junction". Interestingly, an up-regulation trend of HOXA10 protein expression was also observed in NSCLC through tissue chips and immunohistochemistry. In conclusion, the overexpression of HOXA10 may play a pivotal role in the tumorigenesis of NSCLC, and this effect is observed more obviously in LUSC than in LUAD.

Keywords: Homeobox A10, non-small cell lung cancer, tissue samples, qRT-PCR, microarray, RNA sequencing

Introduction

Non-small cell lung cancer (NSCLC) is the most frequently occurring type of malignancy in the lung, representing 80%-85% of lung malignancies [1-5]. Furthermore, the 5-year survival rate of NSCLC is quite low [6-8]. Lung adenocarcinoma (LUAD), lung squamous cell carcinoma (LUSC), and large cell-carcinoma (LC) are the three most common subtypes of NSCLC, with LUAD accounting for about 50%, LUSC for 40%, and LC for 10% of cases among the whole NSCLC population [9-12]. Various biomolecule expression changes have been documented in NSCLC cells [13-15]. For instance, the expression levels of some genes between NSCLC cancer and peri-carcinomatous lung tissues were significantly distinct. Examining the clinical implications of these aberrantly expressed genes may provide new directions for further understanding of NSCLC progression [16-19]. In addition, these differences in gene expression represent potential biomarkers that may function in NSCLC via distinct cellular signaling pathways [20-24]. Consequently, it is important to inquire into the molecular mechanisms of potentially relevant NSCLC tumorigenesis and progression.

Homeobox A10 (HOXA10), also known as PL; HOX1; HOX1H; HOX1.8, locates in 7p15.2 with three exons. Its clinical role and potential

molecular mechanisms have been studied in relation to several diseases, including cancers. Methylation markers in HOXA10 promoter regions have been identified in breast cancer [24]. The HOXA10 promoter CpGs may also predict the survival of breast cancer patients [24]. Overexpression of HOXA10 has been reported in pediatric medulloblastoma cell lines DAOY and ONS-76. In vitro analysis indicates that HOXA10 may influence migration events of medulloblastoma cells but is not crucial for the tumorigenic process of medulloblastoma cells [25]. Silencing the expression of HOXA10 can reverse the multidrug resistance of human chronic mylogenous leukemia K562/ADM cells by affecting p-gp and mrp-1 [26]. Available data suggest that the function of HOXA10 may be tumor specific. The methylation and expression levels of HOXA10 in NSCLC has been investigated in a relatively small number of studies. The methylation of HOXA10 in LUSC has also been studied, and methylation of HOXA10 may represent a prognostic parameter for LUSC patients [27]. In addition, methylation of HOXA10 was observed markedly more frequently in invasive peripheral pulmonary adenocarcinoma (ADC) than in atypical adenomatous hyperplasia (AAH) or adenocarcinoma in situ (AIS) [28]. Only two studies have examined expression levels of HOXA10 in NSCLC. Ludovini et al found that HOXA10 expression was increased in NSCLC based on analysis of 18 patients [29]. Calvo et al reported a similar finding, observing frequent overexpression of HOXA10 in lung cancer cells [30]. However, these reports were based on small sample sizes, and the related molecular mechanism, including the relevant pathways of HOXA10, have not been clarified.

Hence, in the current study, we proposed to investigate the latent value and related signaling pathways of HOXA10 in NSCLC. We analyzed both HOXA10 mRNA and protein levels via multiple detection methods, including in-house quantitative real-time RT-PCR (qRT-PCR), public microarray, RNA sequencing, and tissue chips, as well as through meta-analyses. We further examined the connection between HOXA10 expression and clinicopathological parameters. The inferred relative pathways of HOXA10 were also investigated using various bioinformatic analysis tools.

Materials and methods

Expression level of HOXA10 mRNA by qRT-PCR

A total of 55 patient data with NSCLC were collected (41 males and 14 females; composite life was 66.30 years; range, 33 to 90 years), with both cancerous and adjacent lung tissue obtained through surgery and provided by the Department of Pathology, First Affiliated Hospital of the Guangxi Medical University (Nanning, Guangxi, China), from January 2012 to February 2014. The NSCLC tissue included samples from 23 cases of LUSC and 32 cases of LUAD, as confirmed by pathology. All qRT-PCR procedures were conducted according to the relevant guidelines as previously reported [31]. Total RNA was isolated from the tissue using the Trizol reagent (QIAGEN, Shanghai, China) according to the kit instructions, and a PCR amplification kit (ABI, Life, Technologies, USA) was used. Synthesis of cDNA was implement using the Superscript first strand cDNA synthesis kit (Vazyme Biotech Co., Ltd.) precisely according to the manufacturer's protocol. RT-qPCR was performed using ABI 7500 Prep-Station (Applied Biosystems; Thermo Fisher Scientifi, Inc.), and the SYBR®-Green PCR Master Mix (GeneCore Biotechnologies, Inc., Shanghai, China). PCR was performed first with a 10-min hot start, followed with 95°C for 10 sec, 60°C for 5 sec, and 72°C for 5 sec for 40 cycles. The specific primers used were the following: HOXA10 forward: 5'-CCTTCCGAGAGCAGCAAAG-3', adverse: 5'-CCTTCTCCAGCTCCAGTGTC-3' and GAPDH (internal control) forward, 5'-TGCACCACCAACTGCTTA-3' and reverse, 5'-GGATGCAGGGATGATGTTC-3'. The results were normalized to the GAPDH expression and calculated based on the $2^{-\Delta Cq}$ method. All qRT-PCR reactions and test were repeated at least three times, as previously reported [31-35].

Expression levels of HOXA10 mRNA by RNA-sequencing

We used HOXA10 mRNA expression data for NSCLC and non-cancerous lung tissues taken from the cancer genome atlas (TCGA) and Genotype-Tissue Expression (GTEx) databases. The original data, including HOXA10 expression values and clinical parameters were downloaded for 483 cases of LUAD, 486 cases of LUSC, and 347 and 338 non-cancer cases as controls, respectively. 589 males and 387 females

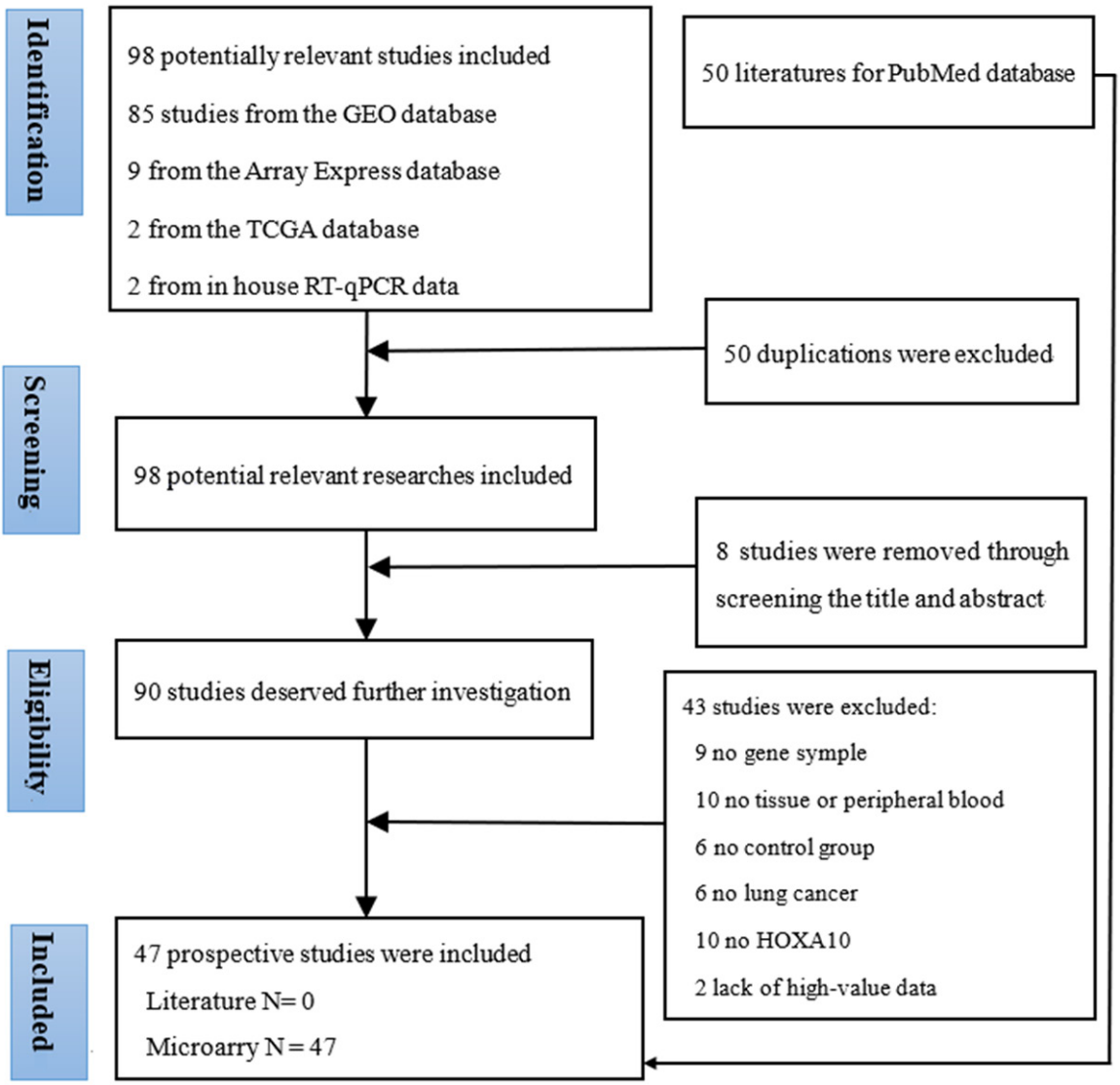

Figure 1. Flow chart of the datasets screened in this investigation.

were included in the current study. Patient ages ranged from 33 to 90, with a median age of 66.3. We used tumor-node-metastasis (TNM) for the classification of malignant tumors and Log2 transfromed for log-scale for the RNA-Seq data, which provided the same results as the analyses we conducted using the online tool GEPIA provided [36]. We also performed survival analysis based on HOXA10 expression levels using overall survival (OS) and disease-free survival (DFS).

Expression level of HOXA10 mRNA by microarray data

In order to notarize the connection between HOXA10 expression levels and NSCLC development and progression, systematic searches were conducted using the Gene Expression Omnibus (GEO), ArrayExpress, Sequence Read Archive (SRA) and Oncomine databases. Search terms used were (lung OR respiration OR pulmonary circulation) AND (cancer OR carcinoma OR tumor OR neoplas* OR malignan*), and the last retrieval was made on Oct 10th, 2018. The filtering process used is shown in **Figure 1**. Essential information including data source, platform, first author, publication year, sample size, and HOXA10 expression level in both cancer and normal control groups was collected for each result selected.

Statistical analysis

All original RNA-Seq data were log 2 transformed. The relationships of HOXA10 expres-

Table 1. Relationship between HOXA10 level and clinicopathological parameters in NSCLC based on qRT-PCR data

Clinicopathological features			N	HOXA10 expression$^{(2-\Delta Cq)}$		
				Mean ± SD	T	*P* value
NSCLC	Tissues	Non-cancerous	55	0.192 ± 0.188	2.139	0.037
		Cancerous	55	0.594 ± 1.380		
	Size	≤ 3	16	0.706 ± 1.432	0.383	0.703
		> 3 cm	39	0.548 ± 1.375		
	TNM	I-II	29	0.758 ± 1.865	0.98	0.335
		III-IV	26	0.411 ± 0.389		
	Gender	Male	41	0.286 ± 0.178	0.966	0.339
		Female	14	0.699 ± 1.586		
	Age	< 60	35	0.565 ± 1.380	-0.205	0.838
		≥ 60	20	0.645 ± 1.414		
	Smoking	No	30	0.270 ± 0.205	-1.79	0.086
		Yes	25	0.983 ± 1.986		
	Vascular invasion	No	50	0.458 ± 0.941	-0.95	0.395
		Yes	5	1.955 ± 3.510		
	LNM	No	29	0.817 ± 0.873	1.345	0.189
		Yes	26	0.345 ± 0.247		
	Grading	I	5	0.246 ± 0.151	F = 0.500	0.61
		II	37	0.728 ± 1.601		
		III	10	0.234 ± 0.150		
LUSC	Tissues	Non-cancerous	23	0.161 ± 0.144	2.052	0.05
		Cancerous	23	0.348 ± 0.413		
	TNM	I-II	10	0.120 ± 0.078	-2.962	0.011
		III-IV	13	0.522 ± 0.481		
LUAD	Tissues	Non-cancerous	32	0.215 ± 0.214	-1.768	0.087
		Cancer	32	0.771 ± 1.766		

sion with clinicopathological parameters in NSCLC were evaluated based on clinical information from TCGA and qRT-PCR. The clinicopathological features data of HOXA10 levels in NSCLC, obtained from qRT-PCR and TCGA, were formulated as mean ± standard deviation (SD). Comparison of HOXA10 expression between two continuous variables was performed using independent samples t-tests. Comparison of two paired variables was calculated using Student's t-test for paired samples. Comparison of more than two different groups was conducted using one-way ANOVA. The clinicopathological features included tissue type, race, age, gender, survival status, Neoplasm Cancer Status, T stage, N stage, M stage and recurrence. The expression pattern and diagnostic capability of HOXA10 for each included dataset was visualized in the form of scatter plots and receiver operating characteristic (ROC) using GraphPad Prism 5 (La Jolla, CA, USA) and SPSS 20.0 (IBM, New York, USA). All statistical analyses were conducted with SPSS 22.0 statistics software (SPSS, Chicago, USA).

Expression level of HOXA10 mRNA by comprehensive meta-analyses

Subgroup analysis of combined standardised mean differences (SMD) and was performed, and the summary receiver operating characteristic curve (SROC) curve and forest plots of sensitivity and specificity were generated by STATA 12.0 (Stata Corporation, TX, USA). The chi-squared-based Cochrane Q-test and I-square (I^2) test were applied to test underlying heterogeneity among the included datasets. When test values indicated no heterogeneity, P > 0.05 and/or I^2 < 50%, a fixed-effects model was applied; otherwise, a random-effects model was used. Deek's funnel plot were used to show potential publication bias [31, 35, 37, 38].

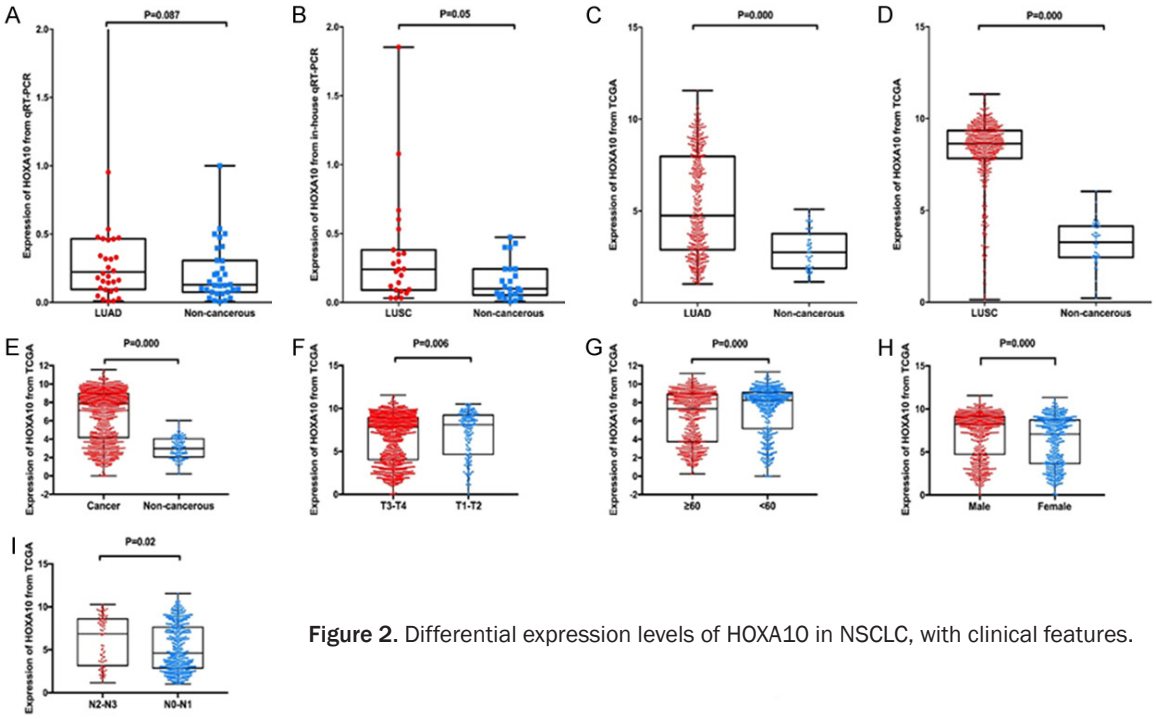

Figure 2. Differential expression levels of HOXA10 in NSCLC, with clinical features.

Co-expressed genes and the signaling pathway related to HOXA10 in NSCLC

The CBioPortal integrates data from 126 tumor genome studies, including large tumor research projects such as TCGA and International Cancer Genome Consortium (ICGC) [39-42]. Co-expressed genes, with correlation coefficients greater than |0.2| in individual cases of LUAD and LUSC were extracted using GEPIA. Junctions of co-expressed genes were computed through the COUNTIF function in Microsoft Excel 2007.

Enrichment analyses of co-expressed genes were conducted utilizing the online tool Web-based Gene Set Analysis Toolkit (WebGestalt). Gene ontology (GO) function analysis and Kyoto Encyclopedia of Genes and Genomes (KEGG) analysis were both incorporated in the mechanism explanation. GO function analysis managed three independent category standards: molecular function (MF), cellular component (CC), and biological process (BP). We defined significative bio-information pathways as $P < 0.05$. Visualization was performed with the R package "GO plot" [43-45].

We used The Search Tool for the Retrieval of Interacting Genes (STRING), a bioinformatics platform and internet resource for identifying and forecasting protein-protein interaction (PPI) networks, as a research instrument for the retrieval of data on the reciprocity of genes/proteins. The current version, STRING 10.5, was used to frame the PPI of proteins which were encoded by the co-expressed genes we extracted. The complete PPI networks and related data were obtained from the STRING online database. The mutual effects and networks among the co-expressed genes were viewed directly via Cytoscape v3.6.1 [46, 47].

Expression level of HOXA10 protein by immunohistochemical staining

The Human Protein Atlas (THPA) includes information for all 24,000 types of tissues and cells relating to human protein distribution [48-50]. Through mining this database, the protein expression of HOXA10 in LUAD and LUSC tissues and in non-cancerous tissues were further verified; the antibody was used antibody CAB019384.

Results

Up-regulation of HOXA10 mRNA by qRT-PCR

We analyzed the differential expression of HOXA10 in 55 NSCLC and para-carcinomatous tissue sample pairs using qRT-PCR (**Table 1**).

Table 2. Relationship between HOXA10 level and clinicopathological parameters in NSCLC based on TCGA data

Clinicopathological features			N	HOXA10 expression$^{(2-\Delta Cq)}$		
				Mean ± SD	T	*P* value
NSCLC	Tissues	Non-cancerous	101	6.7915 ± 2.7498	26.216	0
		Cancer	976	3.0149 ± 1.1390		
	Race	White	882	6.7464 ± 2.7606	F = 1.392	0.249
		Asian	16	6.3519 ± 2.5684		
		Black	78	6.2127 ± 3.0508		
	Age	< 60	389	7.6122 ± 2.33684	8.066	0
		≥ 60	562	6.2366 ± 2.90848		
	Gender	Male	589	7.0204 ± 2.6557	3.515	0
		Female	387	6.3728 ± 2.91544		
	Neoplasm Cancer Status	With tumor	218	7.1328 ± 2.79488	1.577	0.115
		Tumor free	596	6.7897 ± 2.73032		
	Stage	I-II	768	6.7589 ± 2.8029	0.031	0.975
		III-IV	197	6.7521 ± 2.70056		
	M	M0	727	6.9297 ± 2.7508		
		M1	27	6.1930 ± 2.4010		
	T	T1-T2	819	6.6597 ± 2.80573	-2.763	0.006
		T3-T4	154	7.2945 ± 2.57866		
	N	N0-N1	839	6.804 ± 2.77829	1.459	0.145
		N2-N3	121	6.4095 ± 2.79452		
	Recurrence	Recurrence-free	92	6.3499 ± 2.84038	F = 4.341	0.152
		Recurrence	806	6.7898 ± 2.78254		
LUSC	Tissues	Non-cancerous	52	2.8343 ± 1.0876	12.744	0
		Cancer	472	5.3463 ± 2.75696		
	N	N0-N1	386	5.2215 ± 2.74191	-2.327	0.02
		N2-N3	76	6.0276 ± 2.85595		
LUAD	Tissues	Non-cancerous	49	8.1557 ± 1.92362	-17.496	0
		Cancer	504	3.2096 ± 1.17167		

Expression of HOXA10 was significantly up-regulated in the NSCLC tissue of all 55 pairs (0.192 ± 0.188, P = 0.037). HOXA10 was expressed a high level at LUSC (0.348 ± 0.413, P = 0.050, **Figure 2A**). Expression of HOXA10 was increased in advanced LUSC (stage III-IV TNM) (0.522 ± 0.481, P = 0.011) but decreased in early-stage LUSC (stage I-II TNM) (0.120 ± 0.078, P = 0.011). HOXA10 is likely to facilitate the development of LUSC. Results for LUAD were not statistically significant, but we observed a tendency for increased expression of HOXA10 in malignant tissue (**Figure 2B**).

Validation of HOXA10 in NSCLC using RNA-sequencing data

RNA-sequencing data from a total of 976 NSCLC samples. Independent sample t tests showed that HOXA10 expression in TCGA data exhibited significant up-regulation, not only in LUAD (P < 0.001, **Figure 2C**) and LUSC (P < 0.001) (**Figure 2D**) but also in NSCLC (P < 0.001) (**Table 2**, **Figure 2E**). In NSCLC, HOXA10 expression was closely correlated to patient T stage (P = 0.006, **Figure 2F**), age (P < 0.001, **Figure 2G**), gender (P < 0.001, **Figure 2H**). In LUAD, HOXA10 expression was closely correlated to patient N stage (P = 0.02, **Figure 2I**).

Meanwhile, the results of GEPIA also showed that HOXA10 presented a trend of high expression in NSCLC compared to the normal control, in which HOXA10 was overexpressed in LUSC (P < 0.05), as shown in **Figure 3A**. Subsequently, the OS (**Figure 3B**) data from GEPIA conformed to our curve derived from TCGA data, indicating

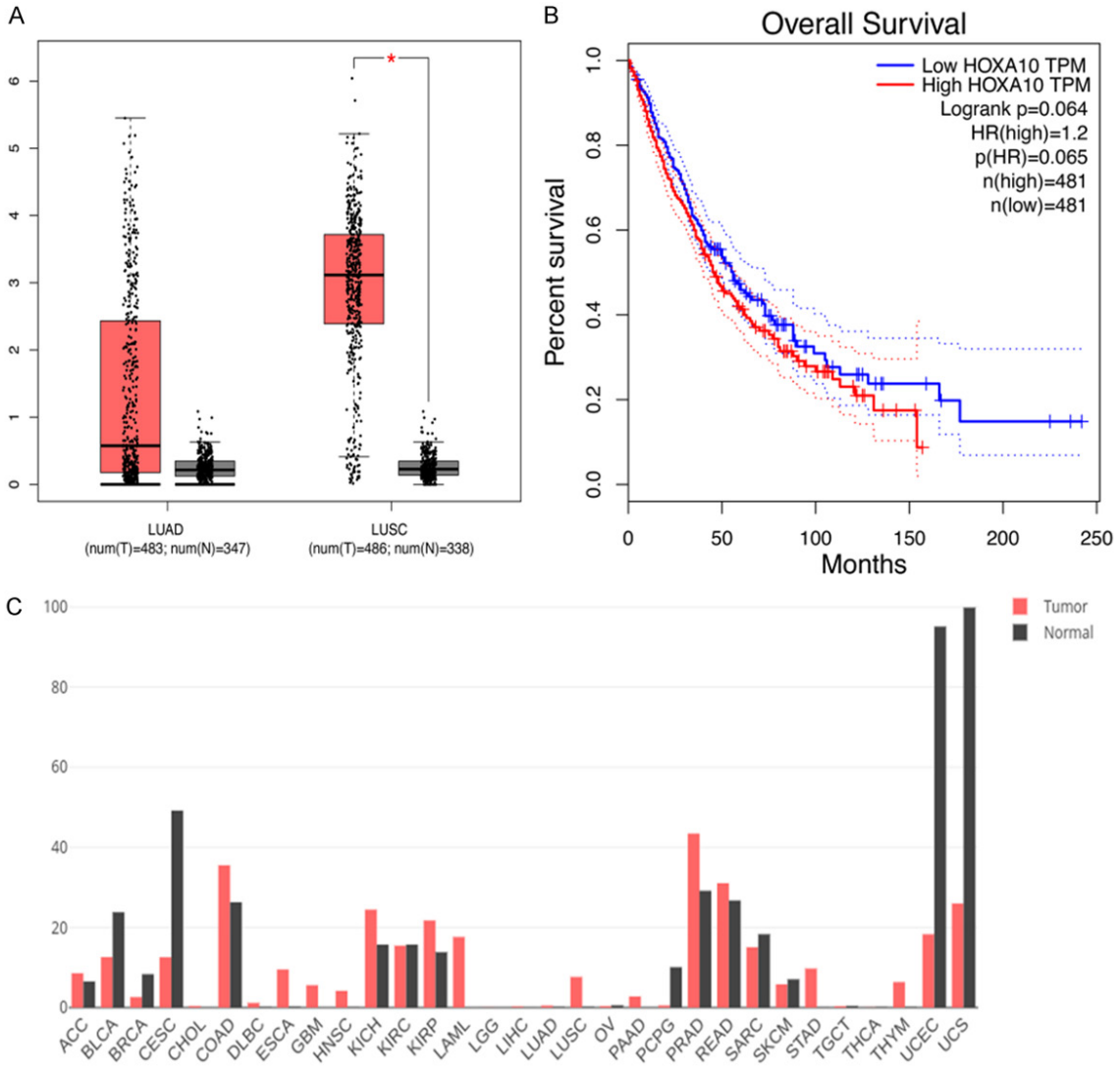

Figure 3. Data for HOXA10 expression levels and KM curves of GEPIA. A. Expressional boxplot of HOXA10 in NSCLC based on GEPIA; B. Kaplan-Meier plots of overall survival (months). C. Expressional regulations of HOXA10 in several cancers based on TCGA and GTEx RNA-sequencing data.

that HOXA10 is associated with survival in NSCLC patients. Finally, we summarized the expression regulations of HOXA10 in pan-cancer (**Figure 3C**).

HOXA10 levels via microarray datasets collected from GEO and ArrayExpress databases

We obtained 43 microarray datasets, which provided HOXA10 expression values for tumor tissue samples (n = 2, 052) and non-tumor tissue samples (n = 1, 169), from the online databases GEO and ArrayExpress. Scatter plots (**Figures 4**, **5**) and ROC curve plots (**Figures 6**, **7**) were created to visually represent the results. Some of the microarrays showed consistent up-regulation of HOXA10 levels in NSCLCs; however, contradictory expression levels were also observed.

Meta-analysis for further verification of the clinical value of HOXA10 in NSCLC

Since the results from individual microarrays were not consistent, we conducted comprehensive systematic meta-analysis of 4,616 cases included in 47 datasets covering data from in-house RT-qPCR, RNA sequencing and all the microarrays. Essential information is shown in **Table 3**. Subgroup analysis of cancer types was

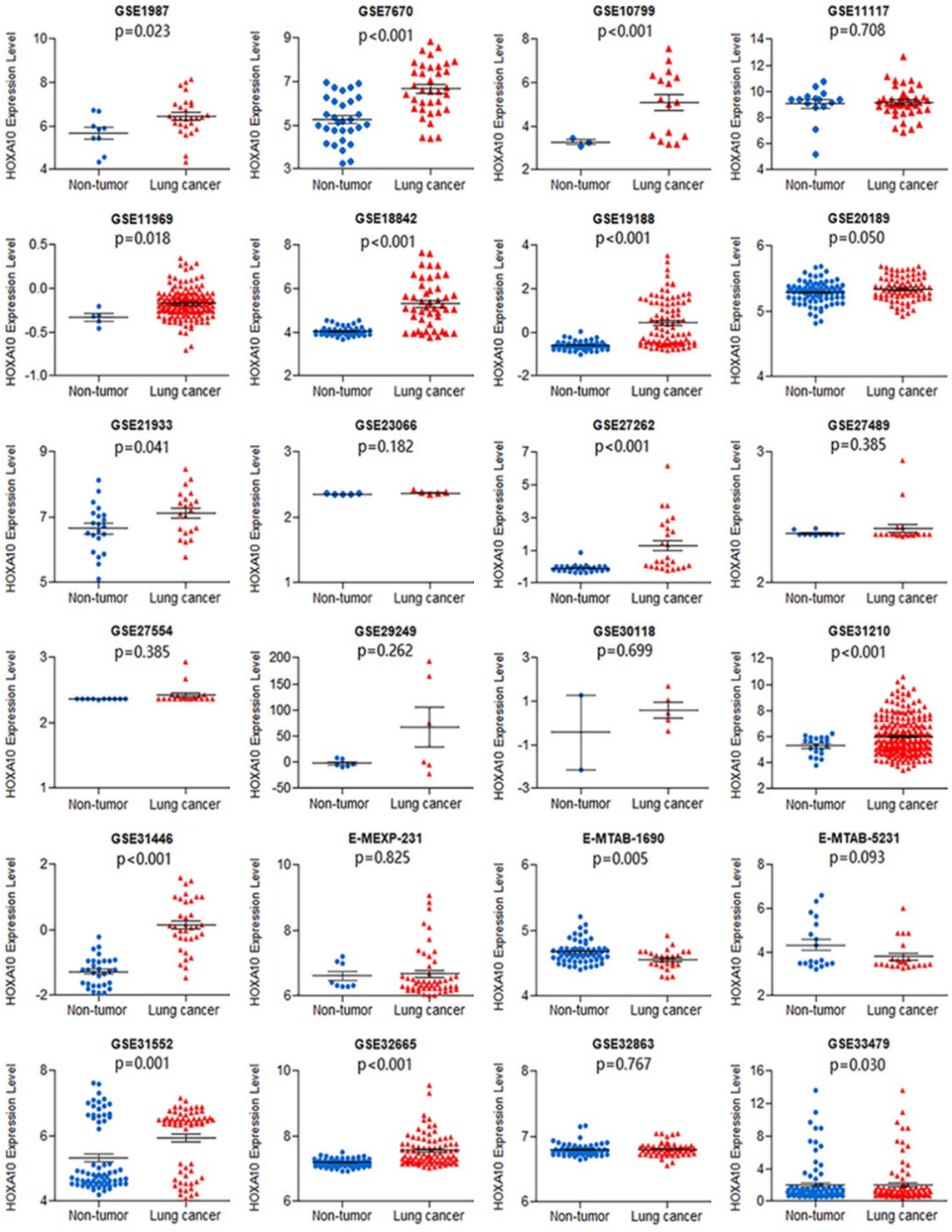

Figure 4. Differences in expression levels of HOXA10 between NSCLC and non-tumor lung tissues based on 24 datasets.

conducted for patients with LUSC, LUAD and NSCLC. The combined SMD value was 0.52 (95% CI: 0.29-0.75, P < 0.001) using the random-effects model (**Figure 8**), indicating that HOXA10 was overexpressed in NSCLC. Another meta-analysis method revealed that the area under the curve (AUC) of SROC was 0.88 (95% CI: 0.81-0.93) for HOXA10 in NSCLC (**Figure**

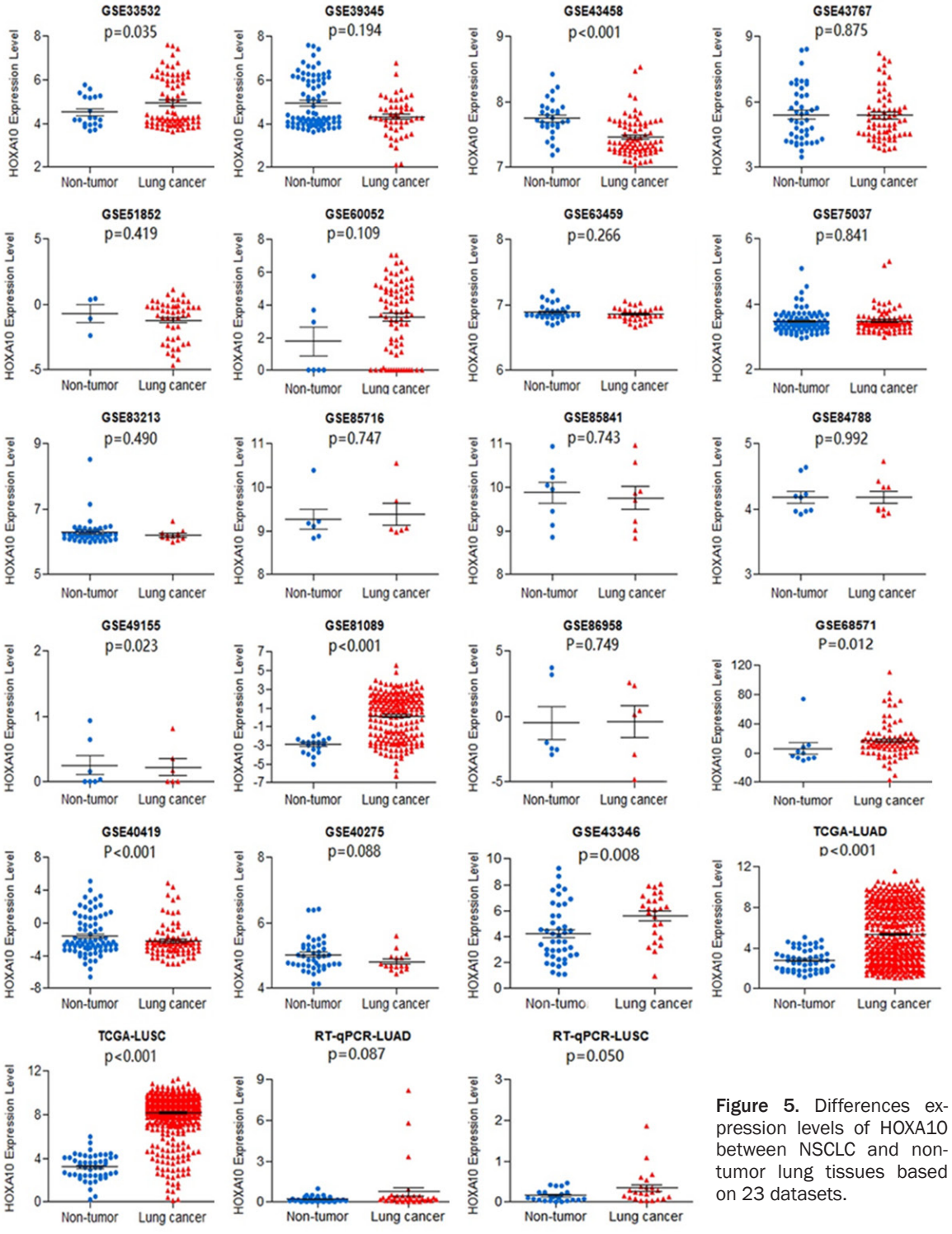

Figure 5. Differences expression levels of HOXA10 between NSCLC and non-tumor lung tissues based on 23 datasets.

9A), with sensitivity and specificity of 0.88 (95% CI: 0.81-0.93) and 0.56 (95% CI: 0.44-0.66), respectively (**Figure 10A**, **10B**). Deek's funnel plot showed publication bias (P = 0.012, **Figure 9B**). The AUC of SROC result for HOXA10 in LUSC and LUAD was 0.86 (95% CI: 0.83-0.89) and 0.75 (95% CI: 0.71-0.78) (**Figure 11A**, **11B**), In addition, The result of publication bias was conducted (LUSC: P = 0.044, LUAD: P = 0.090 **Figure 11C**, **11D**).

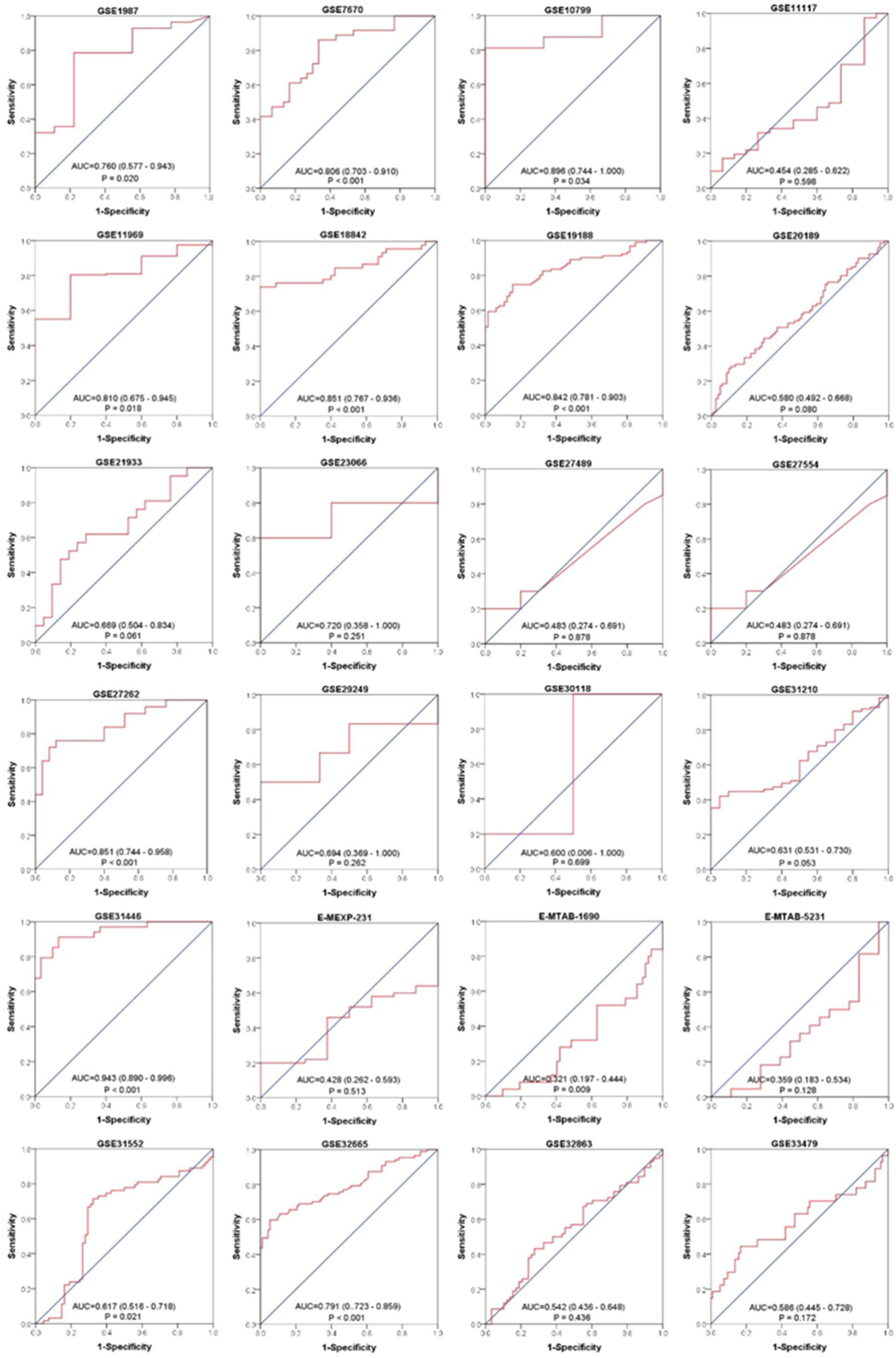

Figure 6. Receiver operating characteristic curves of HOXA10 expression for the differentiation of lung cancer from non-tumor tissues based on 24 datasets.

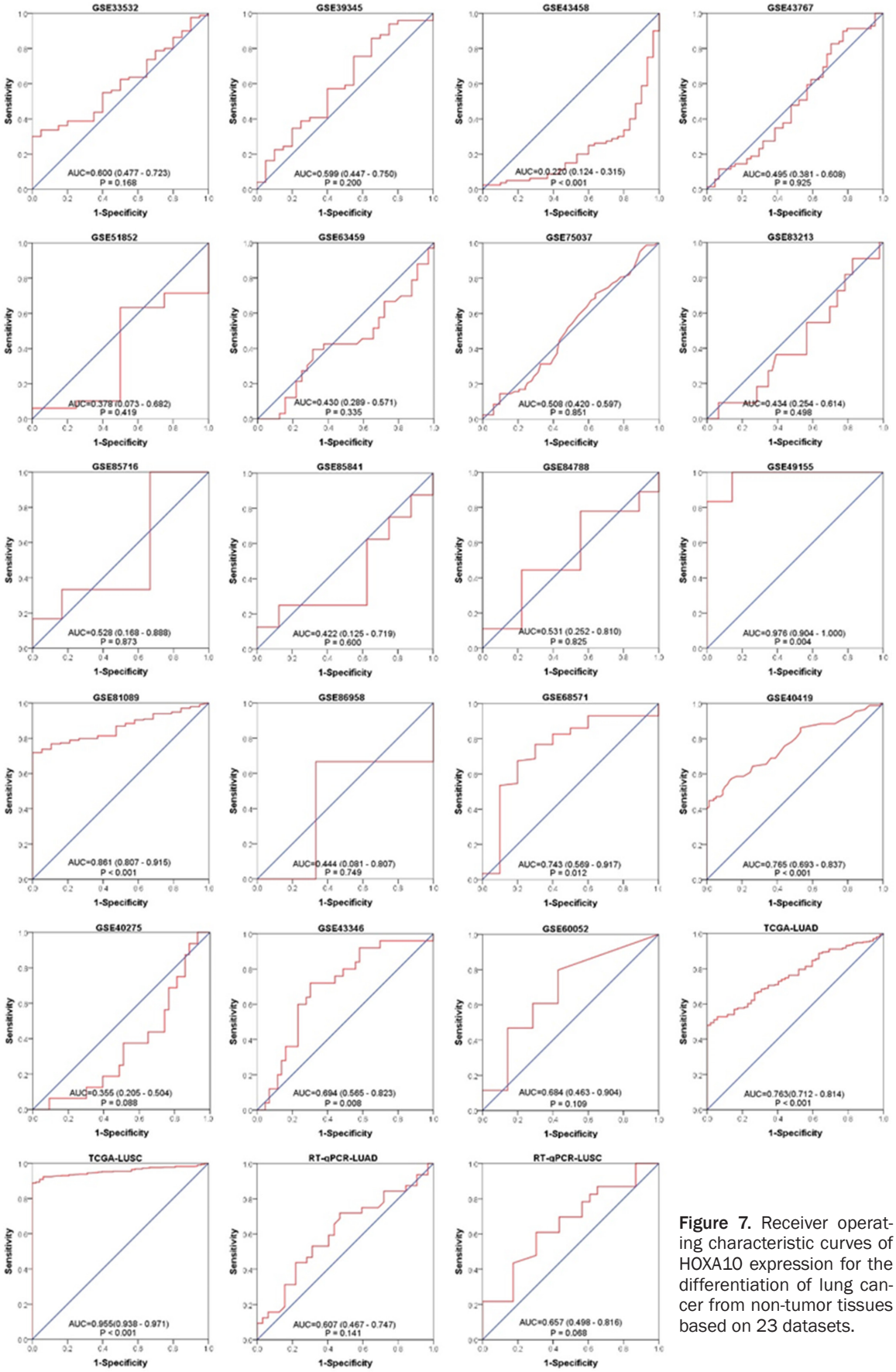

Figure 7. Receiver operating characteristic curves of HOXA10 expression for the differentiation of lung cancer from non-tumor tissues based on 23 datasets.

Table 3. Characteristics of datasets collected from public databases

First author (publication year)	Country	Dataset	Platform	Cancer		Normal	
				N	Mean ± SD	N	Mean ± SD
Kastner S (2012)	Austria	GEO: GSE40275	GPL15974	16	4.811 ± 0.294	43	5.025 ± 0.52
Dehan E (2005)	Israel	GEO: GSE1987	GPL91	28	6.449 ± 0.885	9	5.657 ± 0.827
Baty F (2008)	Switzerland	GEO: GSE11117	GPL6650	41	9.173 ± 1.148	15	9.036 ± 1.343
Takeuchi T (2009)	Japan	GEO: GSE11969	GPL7015	158	-0.176 ± 0.167	5	-0.331 ± 0.092
Ramos AS (2010)	Spain	GEO: GSE18842	GPL570	46	5.307 ± 1.096	45	4.04 ± 0.202
Philipsen S (2010)	Netherlands	GEO: GSE19188	GPL570	91	0.445 ± 1.078	65	-0.601 ± 0.181
Chang J (2013)	Taiwan	GEO: GSE21933	GPL6254	21	7.121 ± 0.708	21	6.652 ± 0.732
Kuner R (2013)	Germany	GEO: GSE23066	GPL570	5	2.372 ± 0.024	5	2.356 ± 0.003
Li-Jen S (2013)	Taiwan	GEO: GSE27262	GPL570	25	1.289 ± 1.662	25	-0.094 ± 0.244
Kuner R (2011)	Germany	GEO: GSE27489	GPL570	20	2.416 ± 0.141	10	2.376 ± 0.019
Kahn N (2011)	Germany	GEO: GSE27554	GPL570	20	2.416 ± 0.141	10	2.376 ± 0.019
Ma L (2012)	China	GEO: GSE29249	GPL10558	6	67.322 ± 92.709	6	-1.942 ± 7.27
Arnaud Muller (2014)	Unknow	Arrayexpress: E-MTAB-1690	GPL570	25	4.561 ± 0.152	62	4.671 ± 0.167
Joerg Mueller (2005)	Unknow	Arrayexpress: E-MTAB-5231	GPL570	22	3.796 ± 0.713	18	4.33 ± 1.134
Marquardt G (2011)	USA	GEO: GSE31552	GPL6244	63	5.942 ± 0.967	68	5.331 ± 1.057
Mascaux C (2011)	USA	GEO: GSE33479	GPL6480	27	5.142 ± 7.057	95	1.987 ± 2.47
Meister M (2011)	Germany	GEO: GSE33532	GPL570	80	4.953 ± 1.132	20	4.517 ± 0.697
Chen Y (2012)	Taiwan	GEO: GSE39345	GPL6104	49	4.332 ± 0.904	20	4.009 ± 0.993
Arima C (2014)	Japan	GEO: GSE51852	GPL6480	49	-1.191 ± 1.521	4	-0.676 ± 1.34
Djureinovic D (2016)	Sweden	GEO: GSE81089	GPL16791	199	0.123 ± 2.387	19	-2.902 ± 1.074
Sato T (2013)	Japan	GEO: GSE43346	GPL570	25	5.618 ± 1.836	43	4.222 ± 2.173
Jiang L (2014)	USA	GEO: GSE60052	GPL11154	79	3.244 ± 2.204	7	1.776 ± 2.374
Nazarov PV (2017)	Luxembourg	GEO: GSE84788	GPL17585	9	4.184 ± 0.286	9	4.185 ± 0.269
Wu H (2011)	USA	GEO: GSE31446	GPL9244	34	0.149 ± 0.791	30	-1.277 ± 0.448
Ooi AT (2013)	USA	GEO: GSE49155	GPL10999	6	0.224 ± 0.321	7	0.226 ± 0.38
TCGA-LUSC (2018)	TCGA	LUSC	NA	500	8.156 ± 1.923	48	3.21 ± 1.172
RT-qPCR (2018)	China	LUSC	NA	23	0.348 ± 0.413	23	0.161 ± 0.149
Su L (2007)	Taiwan	GEO: GSE7670	GPL96	36	6.662 ± 1.208	30	5.253 ± 1.04
Wikman H (2009)	Germany	GEO: GSE10799	GPL570	16	5.089 ± 1.494	3	3.265 ± 0.187
Rotunno M (2011)	USA	GEO: GSE20189	GPL571	81	5.342 ± 0.184	81	5.287 ± 0.171
Ihsan R (2012)	India	GEO: GSE30118	GPL9365	5	0.071 ± 0.396	2	-0.22 ± 2.709
Kohno T (2011)	Japan	GEO: GSE31210	GPL570	226	6.008 ± 1.431	20	5.281 ± 0.7
Antoine Danchin (2005)	Unknow	Arrayexpress: E-MEXP-231	GPL96	50	6.671 ± 0.755	8	6.61 ± 0.399
David Quigley (2013)	USA	GEO: GSE32665	GPL6102	87	7.558 ± 0.473	92	7.191 ± 0.106
Selamat SA (2011)	USA	GEO: GSE32863	GPL6884	58	6.806 ± 0.098	58	6.801 ± 0.097
Kadara H (2013)	USA	GEO: GSE43458	GPL6244	80	7.461 ± 0.289	30	7.75 ± 0.28
Feng L (2013)	China	GEO: GSE43767	GPL6480	69	5.381 ± 1.222	44	5.424 ± 1.26
Robles AI (2014)	USA	GEO: GSE63459	GPL6883	33	6.857 ± 0.101	32	6.887 ± 0.117
Gazdar A (2015)	USA	GEO: GSE75037	GPL6884	83	3.486 ± 0.368	83	3.475 ± 0.347
Bossé Y (2016)	Canada	GEO: GSE83213	GPL10558	11	6.206 ± 0.174	11	6.206 ± 0.174
Duan C (2016)	China	GEO: GSE85716	GPL19612	6	9.388 ± 0.625	6	9.273 ± 0.574
He F (2016)	China	GEO: GSE85841	GPL20115	8	9.757 ± 0.74	8	9.877 ± 0.692
Seo J (2012)	USA	GEO: GSE40419	GPL11154	87	-0.922 ± 2.535	77	-3.01 ± 1.07
Maeda Y (2016)	USA	GEO: GSE86958	GPL16791	6	-0.37 ± 2.946	6	-0.48 ± 3.064
Beer DG (2015)	USA	GEO: GSE68571	GPL80	86	16.751 ± 24.272	10	5.84 ± 24.834
TCGA-LUAD (2018)	TCGA	LUAD	NA	472	5.346 ± 2.757	52	2.834 ± 1.088
RT-qPCR (2018)	China	LUAD	NA	32	0.771 ± 1.766	32	0.215 ± 0.149

Enrichment analysis for ascertaining potential pathways associated with HOXA10 in NSCLC

In total, 111 overlapping, co-expressed genes in LUAD and LUSC were identified using the CBioPortal database. All co-expressed genes were submitted for GO analysis of gene function and KEGG pathway to examine cell signaling pathways. InBP, the co-expressed genes were enriched in "embryonic skeletal system

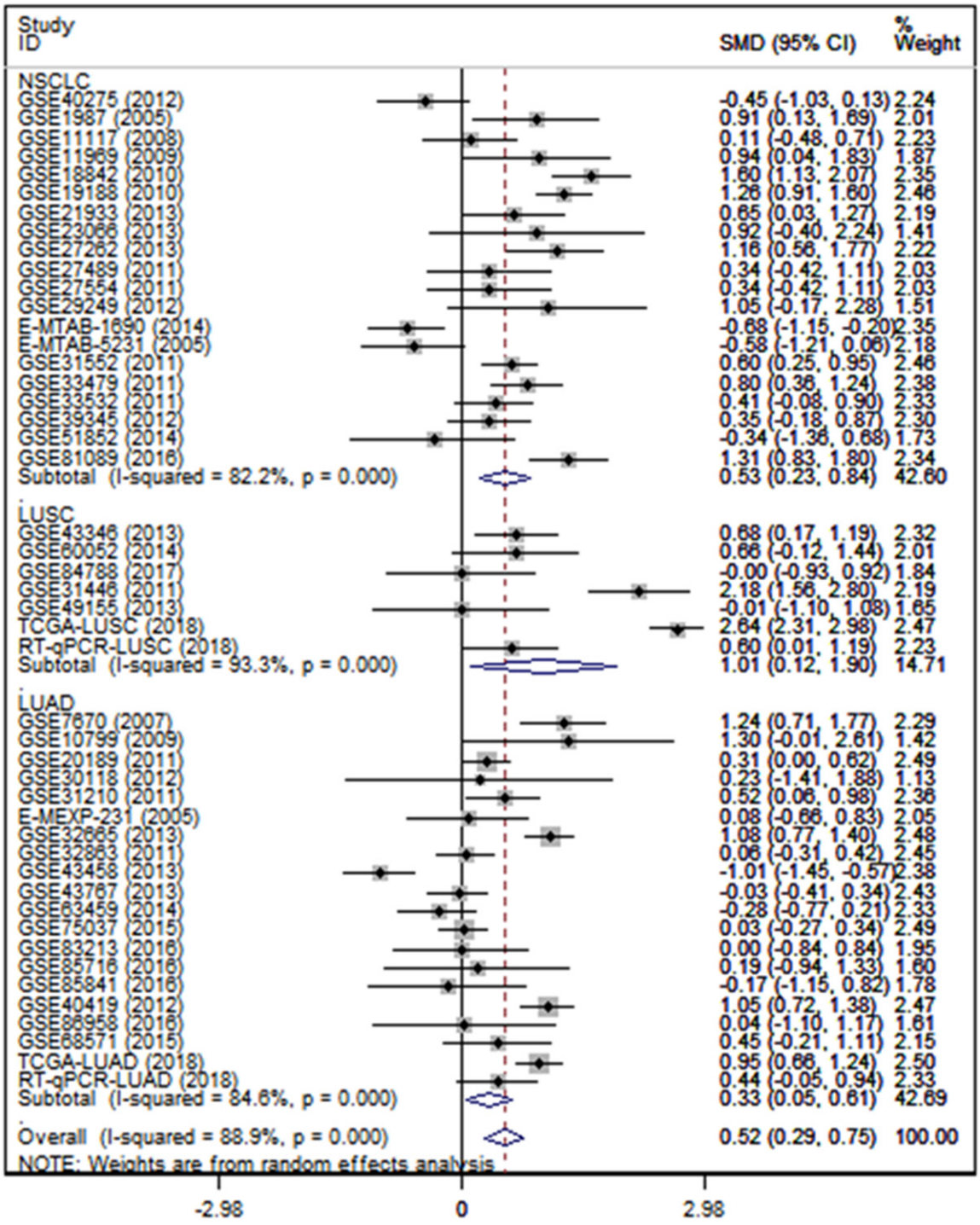

Figure 8. Forest plot evaluating differences in HOXA10 mRNA expression between NSCLC and non-tumor tissues.

development", "embryonic skeletal system morphogenesis" and "regionalization". In CC, the functions of co-expressed genes were concentrated in "extrinsic component of plasma membrane," "extrinsic component of membrane." In MF, the functions of co-expressed genes were enriched in "sequence-specific DNA binding", "transcription factor activity, sequence-specific DNA binding" and "core promoter proximal region DNA binding" (**Figure 12A**). Additionally, the KEGG results showed strong relevance to cancer, including "leuko-

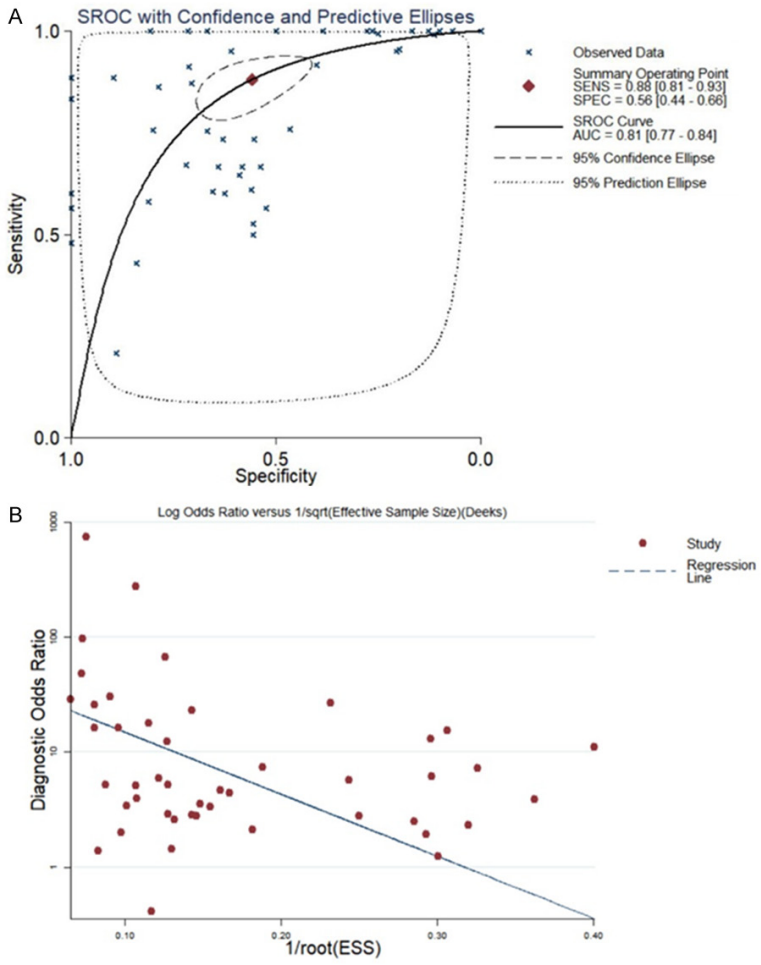

Figure 9. A. SROC curves for the differentiation of NSCLC patients from non-tumor tissues based on HOXA10 expression. B. Result of publication bias.

cyte transendothelial migration", "cell cycle", "primary bile acid biosynthesis", "cell adhesion molecules", "p53 signaling", and "adherens junction" (**Figure 12B**).

Mapping of PPI networks allowed the construction of a landscape showing how the proteins produced by the co-expressed genes interacted with each other. By mapping the whole network, we identified 35 primary hub genes exclusive to the PPI network: HOXA1, HOXA2, HOXA3, HOXA4, HOXA5, HOXA7, HOXA9, HOXB3, CDK1, MLF1IP, ANAPC16, SKP2, CHEK2, DBF4, ANLN, CENPM, RAC1, DNAJC2, CCT6A, GNGT1, AP2M1, SYNJ2, ARRB1, ACTN1, CSK, ORM1, ITGB8, FIGNL, LPIN2, UBN2A, PIF1, RFC2, PJA2, SIAH2, IL6R (**Figure 12C**). Four genes (OCLN, CLDN4, RAC1, ACTN1) appeared in multiple KEGG pathways.

Increased expression of HOXA10 protein by immunohistochemistry (IHC)

Results from IHC staining revealed an up-regulation trend of HOXA10 protein expression in NSCLC, as compared to normal tissue. In some cases of LUSC, expression of HOXA10 was moderately increased (**Figure 13D-F**); in some cases of LUAD, expression of HOXA10 was also moderately increased (**Figure 13G-I**) compared to normal controls. Due to the limited sample size for THPA, no statistics conclusions were possible.

Discussion

Although expression levels of HOXA10 in NSCLC had been reported based on a small number of samples, its clinical significance needed further verification. The mechanism of abnormal expression of HOXA10 in NSCLC was also not clear. To answer these questions, the current study utilized a variety of detecting assays to examine HOXA10 expression levels in NSCLC, including in-house RT-qPCR, RNA sequencing, gene microarray, tissue chips, and immunohistochemistry. In order to comprehensively and objectively investigate the potential role of HOXA10 in the tumorigenesis of NSCLC, we performed meta-analyses, calculating SMD and sROC with the expression data of 4, 616 patients from 47 independent studies. Results from all of the above analytical methods consistently demonstrated increased expression of HOXA10 in NSCLC and its subtypes LUAD and LUSC. We further used in silico method to analyze the pathways of HOXA10-related genes being enriched and found the pathways relating to "cell cycle," "cell adhesion molecules" may be the key pathways through which HOXA10 executes its functions in NSCLC.

To date, only two research groups have conducted studies addressing the clinical signifi-

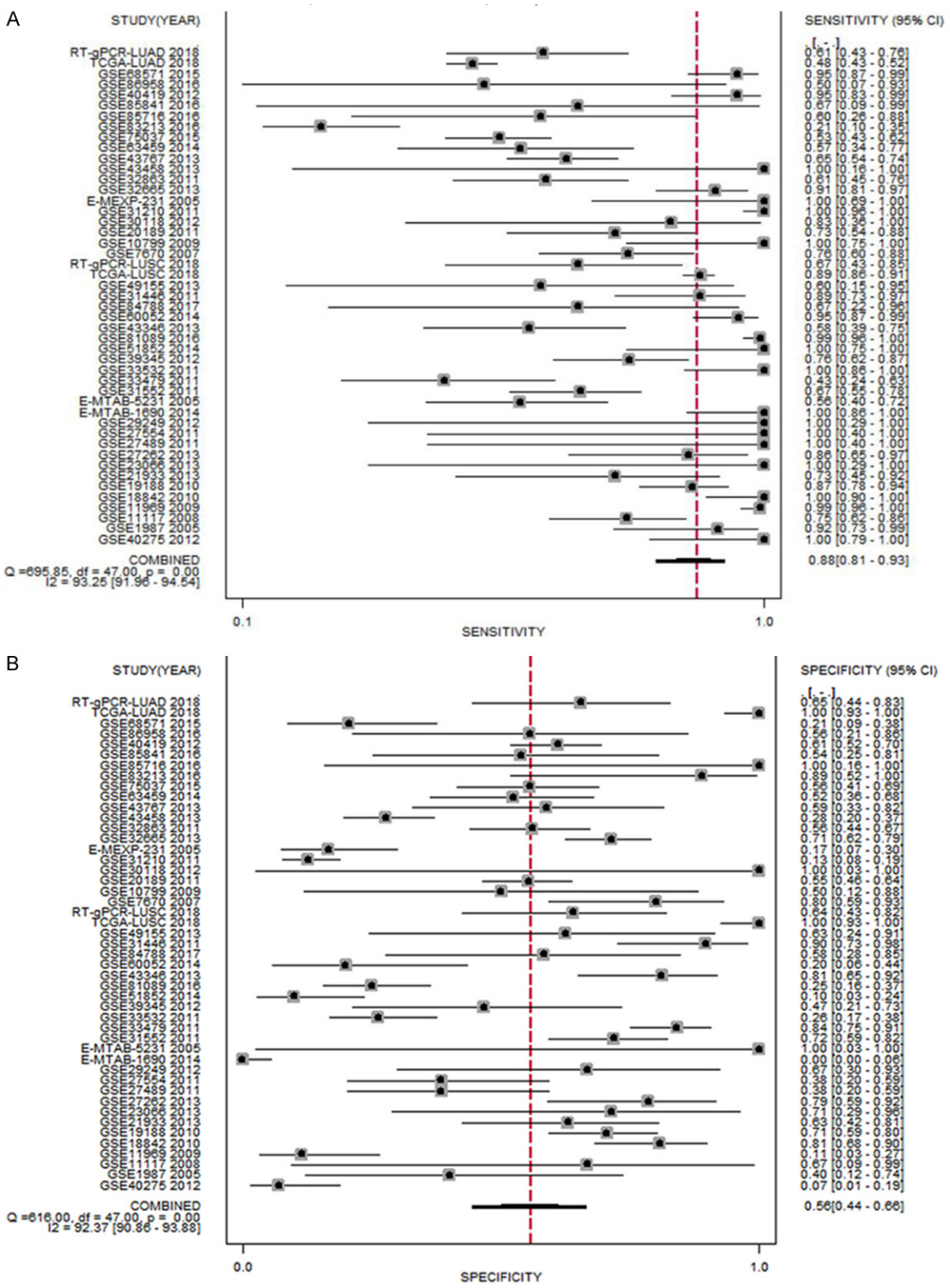

Figure 10. Results of the sensitivity and specificity analysis.

cance of HOXA10 in NSCLC, and both used small sample sizes. Calvo et al [30] detected HOXA10 mRNA expression levels using degenerate qRT-PCR and subsequent real-time quan-

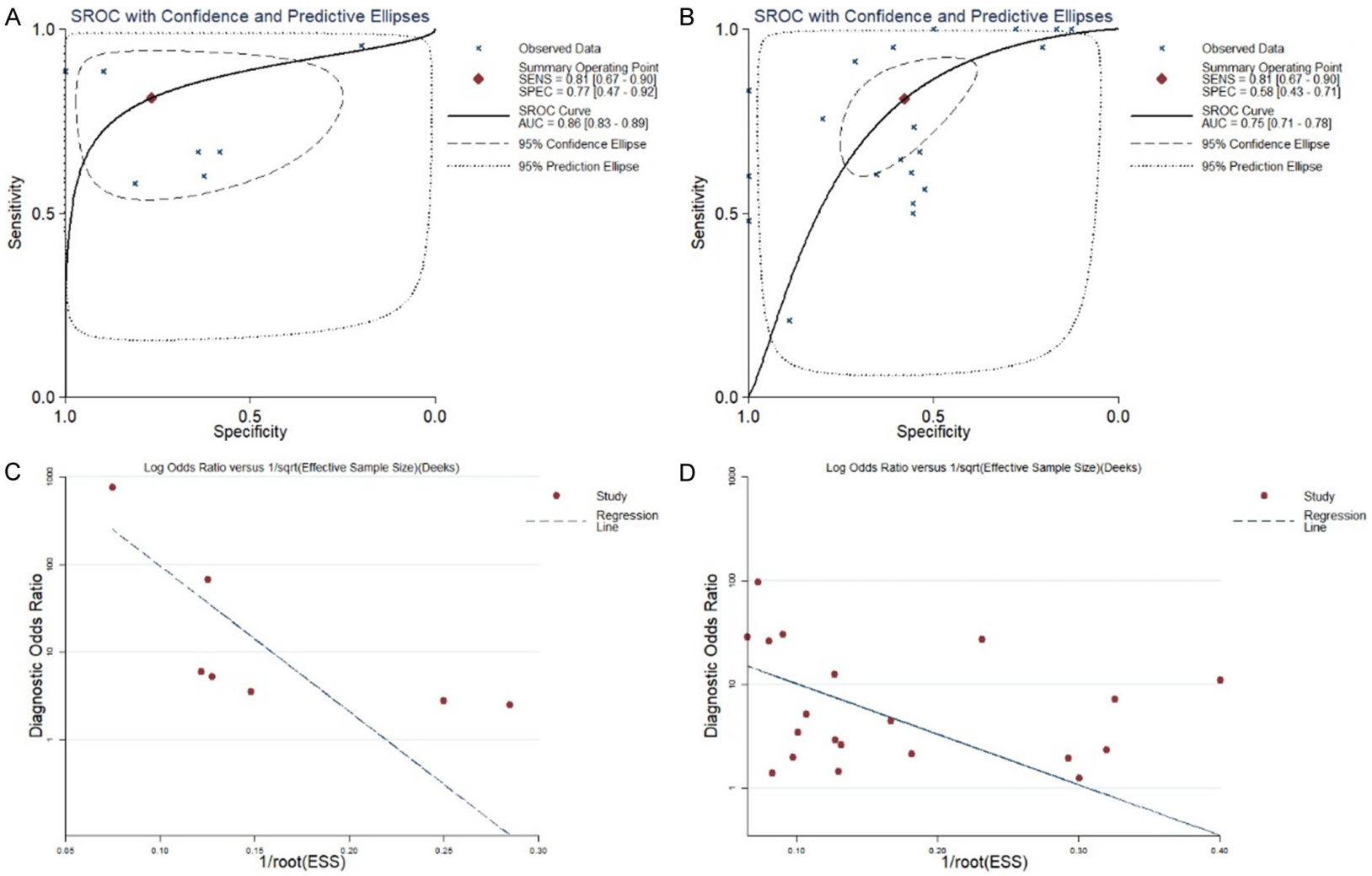

Figure 11. A. SROC curves for the differentiation of LUSC patients from non-tumor tissues based on HOXA10 expression. B. SROC curves for the differentiation of LUAD patients from non-tumor tissues based on HOXA10 expression. C. Deek's funnel plot test of LUSC. D. Deek's funnel plot test of LUAD.

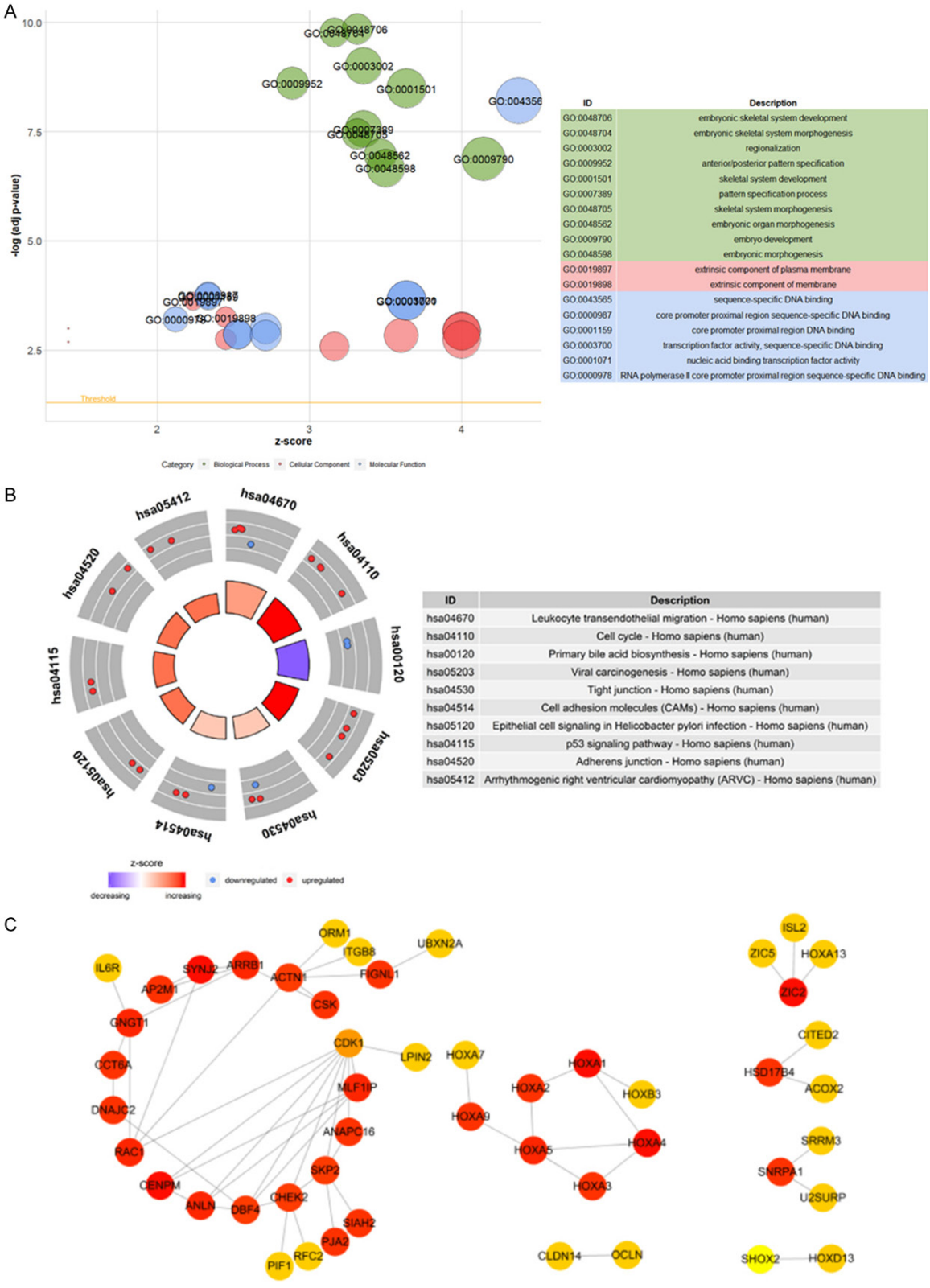

ID	Description
GO:0048706	embryonic skeletal system development
GO:0048704	embryonic skeletal system morphogenesis
GO:0003002	regionalization
GO:0009952	anterior/posterior pattern specification
GO:0001501	skeletal system development
GO:0007389	pattern specification process
GO:0048705	skeletal system morphogenesis
GO:0048562	embryonic organ morphogenesis
GO:0009790	embryo development
GO:0048598	embryonic morphogenesis
GO:0019897	extrinsic component of plasma membrane
GO:0019898	extrinsic component of membrane
GO:0043565	sequence-specific DNA binding
GO:0000987	core promoter proximal region sequence-specific DNA binding
GO:0001159	core promoter proximal region DNA binding
GO:0003700	transcription factor activity, sequence-specific DNA binding
GO:0001071	nucleic acid binding transcription factor activity
GO:0000978	RNA polymerase II core promoter proximal region sequence-specific DNA binding

ID	Description
hsa04670	Leukocyte transendothelial migration - Homo sapiens (human)
hsa04110	Cell cycle - Homo sapiens (human)
hsa00120	Primary bile acid biosynthesis - Homo sapiens (human)
hsa05203	Viral carcinogenesis - Homo sapiens (human)
hsa04530	Tight junction - Homo sapiens (human)
hsa04514	Cell adhesion molecules (CAMs) - Homo sapiens (human)
hsa05120	Epithelial cell signaling in Helicobacter pylori infection - Homo sapiens (human)
hsa04115	p53 signaling pathway - Homo sapiens (human)
hsa04520	Adherens junction - Homo sapiens (human)
hsa05412	Arrhythmogenic right ventricular cardiomyopathy (ARVC) - Homo sapiens (human)

Figure 12. A: Gene ontology analysis of the genes relevant to HOXA10 in NSCLC; B: The significantly enriched annotation of the Kyoto Encyclopedia of Genes and Genomes pathway analysis of the genes relevant to HOXA10 in NSCLC; C: PPI network of co-expression genes of HOXA10 in NSCLC.

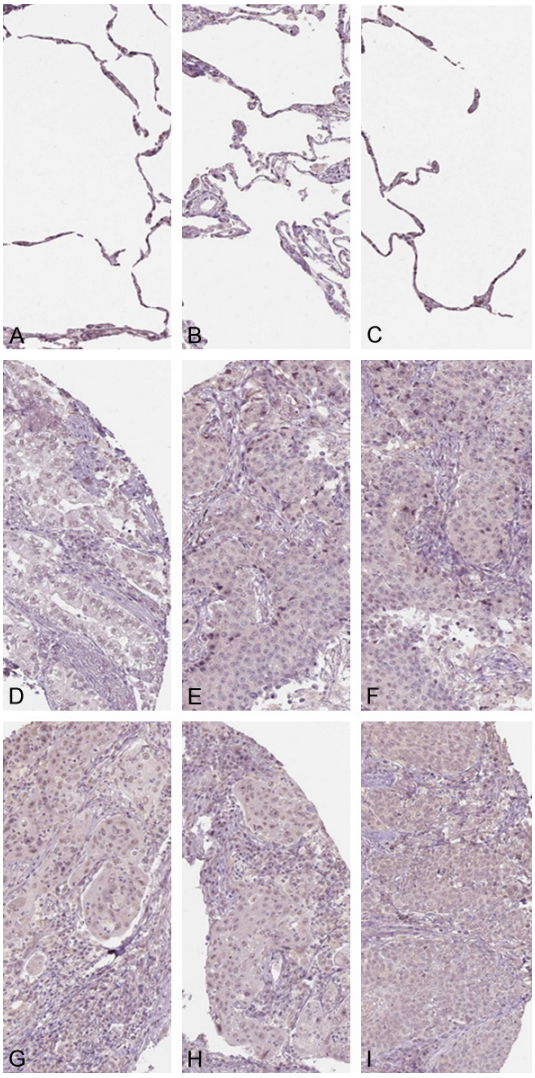

Figure 13. HOXA10 protein expression in LUAD, LUSC and non-tumor tissues assessed by immunohistochemistry. ABC is normal lung tissue; DEF is LUAD tissue; GHI is LUSC tissue.

titative assays for 25 lung cancer cell lines and 25 corresponding tumorous and nonmalignant lung tissue pairs. They found that HOXA10 mRNA was up-regulated in both lung cancer cells and tissues, as compared to non-tumorous lung controls. Ludovini et al [29] did not explore the variation in expression between NSCLC and non-cancerous lung tissue, but they observed the consistent presence of HOXA10 during the development of NSCLC. They focused on the differentially expressed genes in early relapse (ER) compared to no relapse (NR) in resected LUAD patients. Two steps experiments were performed: The first step was a microarray analysis of 18 stage-I LUAD patients (13 cases of NR and 5 cases of ER), from which they identified 50 differentially expressed genes in ER versus NR. In the second step, these 50 genes were detected by q-PCR in an independent cohort of 79 LUAD patients. HOXA10 was one of the coordinate genes which was aberrantly expressed as identified by both microarray and q-PCR. The ER patients presented with significantly increased expression of HOXA10, indicating a potential role of HOXA10 in the development of NSCLC [29]. However, the findings from these two institutes were based on small sample sizes and need to be verified using additional detection methods from multi-centered data with a bigger sample size.

In the current study, several detection approaches were used to investigate the clinical role of HOXA10 in NSCLC tissues. We first performed RT-qPCR using 32 cases of LUAD and 23 cases of LUSC clinical tumor-control pair samples. Consistently, both subtypes of NSCLC showed overexpression of HOXA10 mRNA in LUAD and LUSC. Then RNA-sequencing data from TCGA and GTEx were mined. In 483 cases of LUAD, HOXA10 mRNA showed an up-regulated trend, with levels about three times higher than those of the 347 non-cancerous controls. Meanwhile, in 486 cases of LUSC, significant overexpression was observed, with levels about 15 times higher than those of the 338 controls. We also collected data from GEO and ArrayExpress, and 20 studies with 1, 556 cases of NSCLCs met the inclusion criteria, from which, most of the microarray data showed elevated levels of HOXA10. To comprehensively achieve an overview of HOXA10 mRNA expression in NSCLC, two types of meta-analyses were carried out, and SMD and sROC were calculated simultaneously. The combined SMD from all 47 studies including 4, 616 cases was 0.52 (CI: 0.29-0.75, $P < 0.001$), a result which was strongly supported by the combined AUC of sROC of 0.77 (0.73-0.81). The combined data indicates that HOXA10 plays a more important role in LUSC than in LUAD, as the SMD was 1.01 (CI: 0.12-1.90) in LUSC and 0.33 (CI: 0.05-0.61) in LUAD. Similar results were observed for the AUCs from sROC analyses. Finally, we observed that the HOXA10 protein level appear to be overexpressed in NSCLC tissues. However, the sample size from THPA was quite small, and no statistics calculation was possible. More

analysis using immunohistochemistry is needed to confirm protein levels of HOXA10 in NSCLC. Combined findings from in-house qRT-PCR, RNA-sequencing data, microarray data and meta-analyses of 4, 616 cases clearly indicates up-regulated expression levels of HOXA10, results which are in line with the report of Calvo et al [30]. Thus, the overexpression of HOXA10 may play a pivotal role in the tumorigenesis of NSCLC, and this effect is observed more clearly in LUSC than in LUAD.

Only one study, performed by Ludovini et al [29], showed that HOXA10 mRNA increased more in early relapse lung cancers patients than in those with no relapse. To explore the clinical value of HOXA10 in the development of NSCLC, we attempted to examine the relationship between HOXA10 expression and various clinicopathological parameters. Since no sufficient data were available for a meta-analysis, we analyzed a single cohort from RNA sequencing. Interestingly, LUAD patients with higher level of HOXA10 mRNA tended to have worse overall survival, and HOXA10 mRNA represent an independent risk factor for predicting OS in LUAD patients, with HR being 1.4. When LUAD and LUSC were combined into a NSCLC cohort, HOXA10 still showed potential to predict the OS, with HR of 1.2 ($P = 0.065$). The prognostic value of HOXA10 mRNA in NSCLC is consistent with previous report by Ludovini et al [29], which demonstrates that overexpression of HOXA10 mRNA may accelerate the progression of NSCLC. Nevertheless, the prognostic value of HOXA10 needs further verification with multi-centered data.

Next, we intended to interpret what caused the high expression of HOXA10 in NSCLC and why the high expression of HOXA10 worsens the patient's outcome. It has been reported that marked HOXA10 overexpression was related to elevated fibroblast growth factor 10 (FGF10) and FGF17. During NSCLC development in animal model, the WNT pathway affects cell fate, polarity, and proliferation, and WNT7a has been documented in the maintenance of HOXA10 expression. A homozygous deletion of beta-catenin in the mesothelioma was found to be related to reduced WNT7a and the lowest overall cell line expression of HOXA1, HOXA7, HOXA9, and HOXA10. Hence, alterations in regulatory circuits involving WNT, some HOX family members, including HOXA10, and FGF pathways exist recurrently in NSCLCs [30]. HOXA10 could also function as the target of some non-coding RNAs in lung cancers. A study focusing on a computational framework performed a competing endogenous RNA network construction, which inferred that lncRNA ENSG00000240990 competed with HOXA10 to absorb hsa-let-7a/b/f/g-5p and influence the survival of LUAD patients [51]. In the current study, we inferred the relative signal pathways through which HOXA10 executes its function in NSCLC by collecting co-expressed genes with HOXA10 and performing pathway analysis. The KEGG results showed that the top-ranking pathways included several vital pathways in the development of malignant tumors, such as the pathways of cell cycle, cell adhesion molecules, p53 signaling, and adherens junction, etc. HOXA10 may play a role in the malignant progression of NSCLC by affecting these pathways. The results of PPI also found that HOXA10 is closely linked to some genes. At the same time, it is not surprising that other members of the HOX family and HOXA10 formed a structural loop. Due to the limited reports of mechanism of HOXA10 in NSCLC, more in vitro and in vivo experiments, as well as clinical experiments need to be supplemented.

In summary, this study comprehensively demonstrated the high expression status of HOXA-10 in NSCLC tissues from a variety of examining methods, from mRNA to protein levels. The findings based on 4, 616 cases clearly indicate that high levels of HOXA10 play an important role in tumor formation and progression in NSCLC from individual studies to comprehensive meta-analysis. However, the value of HOXA10 in judging the prognosis in NSCLC patients and the molecular mechanism of its function need further study.

Acknowledgements

The authors thank the TCGA, GTEx, GEO, ArrayExpress and SRA datasets and other bioinformatics tools used in the current study. The presented study was supported by Funds of Natural Science Foundation of Guangxi, China (2017GXNSFAA198016, 2015GXNSFCA139009, 2017GXNSFAA198067), National Natural Science Foundation of China (NSFC 81560469), Guangxi Zhuang Autonomous Region Health and Family Planning Commission Self-financed Scientific Research Project (Z20180979),

Guangxi Medical University Training Program for Distinguished Young Scholars, Medical Excellence Award Funded by the Creative Research Development Grant from the First Affiliated Hospital of Guangxi Medical University.

Disclosure of conflict of interest

None.

Address correspondence to: Kang-Lai Wei and Gang Chen, Department of Pathology, First Affiliated Hospital of Guangxi Medical University, Nanning 530021, Guangxi, Zhuang Autonomous Region, People's Republic of China. E-mail: wklgxmu@163.com (KLW); chengang@gxmu.edu.cn (GC)

References

[1] Qin H, Wang F, Liu H, Zeng Z, Wang S, Pan X and Gao H. New advances in immunotherapy for non-small cell lung cancer. Am J Transl Res 2018; 10: 2234-2245.

[2] Barbareschi M, Barberis M, Buttitta F, Doglioni C, Fiorentino M, Fontanini G, Franco R, Marchetti A, Rossi G and Troncone G. Predictive markers in lung cancer: a few hints for the practicing pathologist. Pathologica 2018; 110: 29-38.

[3] Zinner R, Visseren-Grul C, Spigel DR and Obasaju C. Pemetrexed clinical studies in performance status 2 patients with non-small cell lung cancer (review). Int J Oncol 2016; 48: 13-27.

[4] Pan X, Zhang R, Xie C, Gan M, Yao S, Yao Y, Jin J, Han T, Huang Y, Gong Y, Wang J and Yu B. GRHL2 suppresses tumor metastasis via regulation of transcriptional activity of RhoG in non-small cell lung cancer. Am J Transl Res 2017; 9: 4217-4226.

[5] Zhang Y, Luo J, He R, Huang W, Li Z, Li P, Dang Y, Chen G and Li S. Expression and clinicopathological implication of DcR3 in lung cancer tissues: a tissue microarray study with 365 cases. Onco Targets Ther 2016; 9: 4959-4968.

[6] Testa U, Castelli G and Pelosi E. Lung cancers: molecular characterization, clonal heterogeneity and evolution, and cancer stem cells. Cancers (Basel) 2018; 10.

[7] Zhao J, Shi X, Wang T, Ying C, He S and Chen Y. The prognostic and clinicopathological significance of IGF-1R in NSCLC: a meta-analysis. Cell Physiol Biochem 2017; 43: 697-704.

[8] Li L, Sun Y, Feng M, Wang L and Liu J. Clinical significance of blood-based miRNAs as biomarkers of non-small cell lung cancer. Oncol Lett 2018; 15: 8915-8925.

[9] Lu J, Wang W, Xu M, Li Y, Chen C and Wang X. A global view of regulatory networks in lung cancer: an approach to understand homogeneity and heterogeneity. Semin Cancer Biol 2017; 42: 31-38.

[10] Fernandez-Cuesta L, Perdomo S, Avogbe PH, Leblay N, Delhomme TM, Gaborieau V, Abedi-Ardekani B, Chanudet E, Olivier M, Zaridze D, Mukeria A, Vilensky M, Holcatova I, Polesel J, Simonato L, Canova C, Lagiou P, Brambilla C, Brambilla E, Byrnes G, Scelo G, Le Calvez-Kelm F, Foll M, McKay JD and Brennan P. Identification of circulating tumor DNA for the early detection of small-cell lung cancer. EBioMedicine 2016; 10: 117-123.

[11] Fernandez-Cuesta L and McKay JD. Genomic architecture of lung cancers. Curr Opin Oncol 2016; 28: 52-57.

[12] Gan TQ, Chen WJ, Qin H, Huang SN, Yang LH, Fang YY, Pan LJ, Li ZY and Chen G. Clinical value and prospective pathway signaling of MicroRNA-375 in lung adenocarcinoma: a study based on the cancer genome atlas (TCGA), gene expression omnibus (GEO) and bioinformatics analysis. Med Sci Monit 2017; 23: 2453-2464.

[13] Zhang Y, He RQ, Dang YW, Zhang XL, Wang X, Huang SN, Huang WT, Jiang MT, Gan XN, Xie Y, Li P, Luo DZ, Chen G and Gan TQ. Comprehensive analysis of the long noncoding RNA HOXA11-AS gene interaction regulatory network in NSCLC cells. Cancer Cell Int 2016; 16: 89.

[14] Wang L, Chen Z, An L, Wang Y, Zhang Z, Guo Y and Liu C. Analysis of long non-coding RNA expression profiles in non-small cell lung cancer. Cell Physiol Biochem 2016; 38: 2389-2400.

[15] Huang WT, Cen WL, He RQ, Xie Y, Zhang Y, Li P, Gan TQ, Chen G and Hu XH. Effect of miR146a5p on tumor growth in NSCLC using chick chorioallantoic membrane assay and bioinformatics investigation. Mol Med Rep 2017; 16: 8781-8792.

[16] Watanabe M, Kawaguchi T, Isa SI, Ando M, Tamiya A, Kubo A, Saka H, Takeo S, Adachi H, Tagawa T, Kawashima O, Yamashita M, Kataoka K, Ichinose Y, Takeuchi Y, Watanabe K, Matsumura A and Koh Y. Multiplex ultrasensitive genotyping of patients with non-small cell lung cancer for epidermal growth factor receptor (EGFR) mutations by means of picodroplet digital PCR. EBioMedicine 2017; 21: 86-93.

[17] Akamine T, Toyokawa G, Tagawa T and Seto T. Spotlight on lorlatinib and its potential in the treatment of NSCLC: the evidence to date. Onco Targets Ther 2018; 11: 5093-5101.

[18] Peng W, Wang J, Shan B, Peng Z, Dong Y, Shi W, He D, Cheng Y, Zhao W, Zhang C, Li B and Duan C. Diagnostic and prognostic potential of

circulating long non-coding RNAs in non small cell lung cancer. Cell Physiol Biochem 2018; 49: 816-827.
[19] He RQ, Li XJ, Liang L, Xie Y, Luo DZ, Ma J, Peng ZG, Hu XH and Chen G. The suppressive role of miR-542-5p in NSCLC: the evidence from clinical data and in vivo validation using a chick chorioallantoic membrane model. BMC Cancer 2017; 17: 655.
[20] Iqbal MA, Arora S, Prakasam G, Calin GA and Syed MA. MicroRNA in lung cancer: role, mechanisms, pathways and therapeutic relevance. Mol Aspects Med 2018; [Epub ahead of print].
[21] Chae YK, Arya A, Iams W, Cruz M, Mohindra N, Villaflor V and Giles FJ. Immune checkpoint pathways in non-small cell lung cancer. Ann Transl Med 2018; 6: 88.
[22] Chen WJ, Gan TQ, Qin H, Huang SN, Yang LH, Fang YY, Li ZY, Pan LJ and Chen G. Implication of downregulation and prospective pathway signaling of microRNA-375 in lung squamous cell carcinoma. Pathol Res Pract 2017; 213: 364-372.
[23] Zhang Y, Chen WJ, Gan TQ, Zhang XL, Xie ZC, Ye ZH, Deng Y, Wang ZF, Cai KT, Li SK, Luo DZ and Chen G. Clinical significance and effect of lncRNA HOXA11-AS in NSCLC: a study based on bioinformatics, in vitro and in vivo verification. Sci Rep 2017; 7: 5567.
[24] Park SM, Choi EY, Bae M, Choi JK and Kim YJ. A long-range interactive DNA methylation marker panel for the promoters of HOXA9 and HOXA10 predicts survival in breast cancer patients. Clin Epigenetics 2017; 9: 73.
[25] Bonfim-Silva R, Ferreira Melo FU, Thome CH, Abraham KJ, De Souza FAL, Ramalho FS, Machado HR, De Oliveira RS, Cardoso AA, Covas DT and Fontes AM. Functional analysis of HOXA10 and HOXB4 in human medulloblastoma cell lines. Int J Oncol 2017; 51: 1929-1940.
[26] Yi YJ, Jia XH, Wang JY, Li YJ, Wang H and Xie SY. Knockdown of HOXA10 reverses the multidrug resistance of human chronic mylogenous leukemia K562/ADM cells by downregulating P-gp and MRP-1. Int J Mol Med 2016; 37: 1405-1411.
[27] Heller G, Babinsky VN, Ziegler B, Weinzierl M, Noll C, Altenberger C, Mullauer L, Dekan G, Grin Y, Lang G, End-Pfutzenreuter A, Steiner I, Zehetmayer S, Dome B, Arns BM, Fong KM, Wright CM, Yang IA, Klepetko W, Posch M, Zielinski CC and Zochbauer-Muller S. Genome-wide CpG island methylation analyses in non-small cell lung cancer patients. Carcinogenesis 2013; 34: 513-521.
[28] Chung JH, Lee HJ, Kim BH, Cho NY and Kang GH. DNA methylation profile during multistage progression of pulmonary adenocarcinomas. Virchows Arch 2011; 459: 201-211.
[29] Ludovini V, Bianconi F, Siggillino A, Piobbico D, Vannucci J, Metro G, Chiari R, Bellezza G, Puma F, Della Fazia MA, Servillo G and Crino L. Gene identification for risk of relapse in stage I lung adenocarcinoma patients: a combined methodology of gene expression profiling and computational gene network analysis. Oncotarget 2016; 7: 30561-30574.
[30] Calvo R, West J, Franklin W, Erickson P, Bemis L, Li E, Helfrich B, Bunn P, Roche J, Brambilla E, Rosell R, Gemmill RM and Drabkin HA. Altered HOX and WNT7A expression in human lung cancer. Proc Natl Acad Sci U S A 2000; 97: 12776-12781.
[31] Gan BL, He RQ, Zhang Y, Wei DM, Hu XH and Chen G. Downregulation of HOXA3 in lung adenocarcinoma and its relevant molecular mechanism analysed by RT-qPCR, TCGA and in silico analysis. Int J Oncol 2018; 53: 1557-1579.
[32] Yang X, Deng Y, He RQ, Li XJ, Ma J, Chen G and Hu XH. Upregulation of HOXA11 during the progression of lung adenocarcinoma detected via multiple approaches. Int J Mol Med 2018; 42: 2650-2664.
[33] Zhang R, Zhang TT, Zhai GQ, Guo XY, Qin Y, Gan TQ, Zhang Y, Chen G, Mo WJ and Feng ZB. Evaluation of the HOXA11 level in patients with lung squamous cancer and insights into potential molecular pathways via bioinformatics analysis. World J Surg Oncol 2018; 16: 109.
[34] Zhang Y, Li XJ, He RQ, Wang X, Zhang TT, Qin Y, Zhang R, Deng Y, Wang HL, Luo DZ and Chen G. Upregulation of HOXA1 promotes tumorigenesis and development of nonsmall cell lung cancer: a comprehensive investigation based on reverse transcription-quantitative polymerase chain reaction and bioinformatics analysis. Int J Oncol 2018; 53: 73-86.
[35] Deng Y, He R, Zhang R, Gan B, Zhang Y, Chen G and Hu X. The expression of HOXA13 in lung adenocarcinoma and its clinical significance: a study based on the cancer genome atlas, oncomine and reverse transcription-quantitative polymerase chain reaction. Oncol Lett 2018; 15: 8556-8572.
[36] Tang Z, Li C, Kang B, Gao G, Li C and Zhang Z. GEPIA: a web server for cancer and normal gene expression profiling and interactive analyses. Nucleic Acids Res 2017; 45: W98-W102.
[37] Liang YY, Huang JC, Tang RX, Chen WJ, Chen P, Cen WL, Shi K, Gao L, Gao X, Liu AG, Peng XT, Chen G, Huang SN, Fang YY and Gu YY. Clinical value of miR-198-5p in lung squamous cell carcinoma assessed using microarray and RT-qPCR. World J Surg Oncol 2018; 16: 22.

[38] Biaoxue R, Hua L, Wenlong G and Shuanying Y. Increased serum amyloid a as potential diagnostic marker for lung cancer: a meta-analysis based on nine studies. BMC Cancer 2016; 16: 836.

[39] Gao J, Aksoy BA, Dogrusoz U, Dresdner G, Gross B, Sumer SO, Sun Y, Jacobsen A, Sinha R, Larsson E, Cerami E, Sander C and Schultz N. Integrative analysis of complex cancer genomics and clinical profiles using the cBioPortal. Sci Signal 2013; 6: pl1.

[40] Gao L, Zhong JC, Huang WT, Dang YW, Kang M and Chen G. Integrative analysis of BSG expression in NPC through immunohistochemistry and public high-throughput gene expression data. Am J Transl Res 2017; 9: 4574-4592.

[41] Meng J, Wang LH, Zou CL, Dai SM, Zhang J and Lu Y. C10orf116 gene copy number loss in prostate cancer: clinicopathological correlations and prognostic significance. Med Sci Monit 2017; 23: 5176-5183.

[42] Wang Q, Li Z, Wu Y, Huang R, Zhu Y, Zhang W, Wang Y and Cheng J. Pharmacological inhibition of Bmi1 by PTC-209 impaired tumor growth in head neck squamous cell carcinoma. Cancer Cell Int 2017; 17: 107.

[43] Guo W, Zhang B, Li Y, Duan HQ, Sun C, Xu YQ and Feng SQ. Gene expression profile identifies potential biomarkers for human intervertebral disc degeneration. Mol Med Rep 2017; 16: 8665-8672.

[44] Gong AX, Zhang JH, Li J, Wu J, Wang L and Miao DS. Comparison of gene expression profiles between dental pulp and periodontal ligament tissues in humans. Int J Mol Med 2017; 40: 647-660.

[45] Yan M, Song M, Bai R, Cheng S and Yan W. Identification of potential therapeutic targets for colorectal cancer by bioinformatics analysis. Oncol Lett 2016; 12: 5092-5098.

[46] Liang L, Wei DM, Li JJ, Luo DZ, Chen G, Dang YW and Cai XY. Prognostic microRNAs and their potential molecular mechanism in pancreatic cancer: a study based on the cancer genome atlas and bioinformatics investigation. Mol Med Rep 2018; 17: 939-951.

[47] He RQ, Zhou XG, Yi QY, Deng CW, Gao JM, Chen G and Wang QY. Prognostic signature of alternative splicing events in bladder urothelial carcinoma based on spliceseq data from 317 cases. Cell Physiol Biochem 2018; 48: 1355-1368.

[48] Uhlen M, Fagerberg L, Hallstrom BM, Lindskog C, Oksvold P, Mardinoglu A, Sivertsson A, Kampf C, Sjostedt E, Asplund A, Olsson I, Edlund K, Lundberg E, Navani S, Szigyarto CA, Odeberg J, Djureinovic D, Takanen JO, Hober S, Alm T, Edqvist PH, Berling H, Tegel H, Mulder J, Rockberg J, Nilsson P, Schwenk JM, Hamsten M, von Feilitzen K, Forsberg M, Persson L, Johansson F, Zwahlen M, von Heijne G, Nielsen J and Ponten F. Proteomics. Tissue-based map of the human proteome. Science 2015; 347: 1260419.

[49] Thul PJ, Akesson L, Wiking M, Mahdessian D, Geladaki A, Ait Blal H, Alm T, Asplund A, Bjork L, Breckels LM, Backstrom A, Danielsson F, Fagerberg L, Fall J, Gatto L, Gnann C, Hober S, Hjelmare M, Johansson F, Lee S, Lindskog C, Mulder J, Mulvey CM, Nilsson P, Oksvold P, Rockberg J, Schutten R, Schwenk JM, Sivertsson A, Sjostedt E, Skogs M, Stadler C, Sullivan DP, Tegel H, Winsnes C, Zhang C, Zwahlen M, Mardinoglu A, Ponten F, von Feilitzen K, Lilley KS, Uhlen M and Lundberg E. A subcellular map of the human proteome. Science 2017; 356.

[50] Uhlen M, Zhang C, Lee S, Sjostedt E, Fagerberg L, Bidkhori G, Benfeitas R, Arif M, Liu Z, Edfors F, Sanli K, von Feilitzen K, Oksvold P, Lundberg E, Hober S, Nilsson P, Mattsson J, Schwenk JM, Brunnstrom H, Glimelius B, Sjoblom T, Edqvist PH, Djureinovic D, Micke P, Lindskog C, Mardinoglu A and Ponten F. A pathology atlas of the human cancer transcriptome. Science 2017; 357.

[51] Wei Y, Yan Z, Wu C, Zhang Q, Zhu Y, Li K and Xu Y. Integrated analysis of dosage effect lncRNAs in lung adenocarcinoma based on comprehensive network. Oncotarget 2017; 8: 71430-71446.